International Journal of Current Engineering and Technology
E-ISSN 2277 – 4106, P-ISSN 2347 – 5161

Available at http://inpressco.com/category/ijcet

Research Article

Phase Evaluation, microscopy and Band gap of Fe-doped nanocrystalline $BaSnO_3$ by Solid-Sate Sintering assisted with agate-mortar activation

Asima Adak (Maity)†, Soumya Mukherjee‡*, Mahua Ghosh Chaudhuri#, Tamali Chakraborty‡ and Siddhartha Mukherjee‡

†Department of Electronics & Communication Engineering, Heritage Institute of Technology, Kolkata-700107, India
‡Department of Metallurgical & Materials Engineering, Jadavpur University, 188, Raja S.C. Mallick Road, Kolkata-700032, India
#School of Material Science and Nanotechnology, Jadavpur University, 188, Raja S.C. Mallick Road, Kolkata-700032, India

Accepted 18 Dec 2015, Available online 20 Dec 2015, **Vol.5, No.6 (Dec 2015)**

Abstract

Iron (Fe) doped barium stannate ($BaSn_{1-x}Fe_xO_3$) with x= 0.05, 0.10 and 0.15 were prepared by mechanical mixing in agate mortar followed by sintering at 1350^{0}C for 2 hours. X-ray diffraction analysis (XRD) of the synthesized sample confirmed the major phases to be cubic perovskite structure, crystallite size by Scherrer's formula and planes of orientation of the peaks along directions having minimum energy leading to thermodynamic stability of the phases developed. Absorption due to symmetric and asymmetric stretching of inorganic bond formation for the required M-O coordination was determined by Fourier transform infrared spectroscopy (FTIR). Band gap analyses of the sintered samples were carried out by UV-VIS using Tauc plot. Morphological studies were carried out by SEM, FESEM while EDX analysis was done to verify the presence of required elements in the matrix of the synthesized samples.

Keywords: *Perovskite-Spinel, PL spectra, Dielectric, P-E loop.*

1. Introduction

Barium Stannate ($BaSnO_3$) is a type of ceramic material with cubic perovskite structure which has many important applications in material science and technology due to their dielectric, electro optical and magnetic properties. It can be applied as a material for thermally stable capacitor and to fabricate ceramic boundary layer capacitor (Upadhay Shail *et. al*, Kocemba I *et. al.*, Lu Wensheng *et. al.*). $BaSnO_3$ material can also be used for humidity sensor (Upadhay Shail *et. al*), semiconductor gas sensor and photocatalytic applications (Köferstein, Roberto *et. al*) due to its defect and structural aspects. $BaSnO_3$ is an n-type semiconducting material with optical bandgap of 3.1eV (James K.K *et. al.*). The optical bandgap reported for thin film of La doped $BaSnO_3$ is in the visible region with value about 4.02eV when it is deposited on MgO substrate(James K.K *et. al.*, Wei, Xiaoyong *et. al.*). Doped and undoped $BaSnO_3$ has a simple cubic perovskite type structure. Difference in the ionic radii of the Sn^{4+} and Fe^{2+} ions produces lattice strain resulting in increase on lattice constant (James K.K *et. al.*, Upadhay Shail & Om Prakash *et. al.*). It have been reported by some researchers that this category of ceramic material exhibits strong near- infrared luminescence at room temperature (Lu Wensheng *et. al.*, Wei, Xiaoyong *et. al.*). $BaSnO_3$ can also be put into use for photoelectrochemical applications since the band gap (3.1eV to 3.4 eV) is noted to be similar to some important materials like TiO_2, ZnO, $SrTiO_3$ which act as hydrogen photo catalyst (8). The material is found to be stable at temperature up to 1273K and above (Bouhemadou, A *et. al.*, Kocemba I *et. al.*). In spite of having higher sintering temperature, samples of cubic Barium Stannate sintered at above 1600^{0}C is noted to have porous morphology (Wei Xiaoyong. *et. al.*, Singh Prabhakar *et. al.*).

Till now, very few research articles are still found to be dedicated to structural aspects, optical properties of Fe doped nanocrystalline Barium Stannate by mechanical agate-mortar activated solid-state route sintering while in contrast research articles on complex route synthesis is available. This method of approach for synthesis is relatively an easy economically effective process of synthesizing nanomaterials. The detail characterization studies are carried out by XRD for phase identification, SEM /EDX for morphology, size analysis of the particle, elemental compositional analysis and FTIR for bond formation in relation to M-O co-ordination. Band gap, optical

*Corresponding address: **Soumya Mukherjee**, Mobile: 919830179414, At Present: Assistant Professor, Amity School of Engineering and Technology, Amity University Kolkata Campus, Kolkata-700156, West Bengal, India

properties of Fe doped $BaSnO_3$ are also measured from UV-VIS spectra of the synthesized sample.

2. Experimental details

Fe doped $BaSnO_3$ with different percentage of Fe ($BaSn_{1-x}Fe_xO_3$, where x= 0.05, 0.10 and 0.15) were prepared by mechanical mixing in agate mortar followed by sintering method**.** Stoichiometric amounts of BaO, SnO_2 and Fe_2O_3 were mixed using agate mortar and pestle for 3 hours with initial starting material of pure $BaCO_3$, SnO_2 and Fe_2O_3 (Merck India, Ltd). The $BaCO_3$ was decomposed at 1250^0C to obtain pure BaO. Then mixed powders were dried and sintered at 1350^0C for 2 hours in tubular furnace maintaining air as atmosphere. The sintered samples were characterized by X-ray diffractometer (Rigaku, Ultima III) using Cu source having wave length λ = 1.54Å with slow scan speed of 5^0/min within the scan range of 10-80˚. Crystalline size was determined using Scherrer's relation t=0.9λ/cosθ where t is the crystallite size, λ is the wavelength used. The sample composition was analyzed by EDX (using ultra Dry Silicon Drift Detector from Thermo Scientific) to clarify doping of Fe within barium stannate by identifying the peaks Fe, Ba, Sn and O. Morphological studies were observed by both SEM and FESEM (Hitachi, S-4800). Stretching and vibration of M-O coordinations were characterized by FTIR (FTIR Shimadza, IR- 21 prestige) from the absorption bands within scan range of 5000-400cm^{-1}. For FTIR analysis, sample was mixed with KBr and pellets are formed in steel die having diameter of 10mm under pressure of 6tonne/cm^2. For UV-VIS analysis, sample was sonicated in deionized water for about 1 hour till clear solution was observed and scanning of spectra was carried in the range of 150-750cm. Absorption spectra and band gap were evaluated using Tauc relation from spectra, using UV-VIS spectrophotometer (Perkin Elmer, Lambda 35).

3. Results and discussion

3.1. Phase determination of the powder by XRD analysis

X-ray diffraction pattern of Fe doped barium stannate sintered at 1350^0C for 2 hours with different composition is shown in Fig 1 to Fig 3. It has been observed that all the peaks are assigned to a single phase cubic structure. All these directional planes along (110), (111), (200), (211), (220) and (310) are cubic perovskite of $BaSnO_3$ matched with ICDD-JCPDS PDF# 150780 (Omeiri S *et. al.*). Crystallite size of this powder sample is determined by Debye-Scherrer formula t= 0.9λ/βcosθ where "t" is the crystallite size, λ is the wavelength of the X-rays used, β is the broadening of diffraction line measured at the half of its maximum intensity in radians and θ is the angle of diffraction (Cullity B D). The variation of crystallite size with different composition of Fe doped $BaSnO_3$ is very small (James K.K. *et. al.*). The average crystallite size is 49.12 nm (Lu Wensheng *et. al.*) 2θ position of undoped BaSN sample is 30.68° while for doped sample it shifts negligibly to 30.61° 30.807° for 10% Fe doped, 5, and 15% doped samples. The slight shift indicates strain induced at the lattice position of B site of perovskite ABO_3. In the present case B site is occupied by Sn for undoped while partially by Fe at Sn site causing strain and shift of the main crystalline peak.

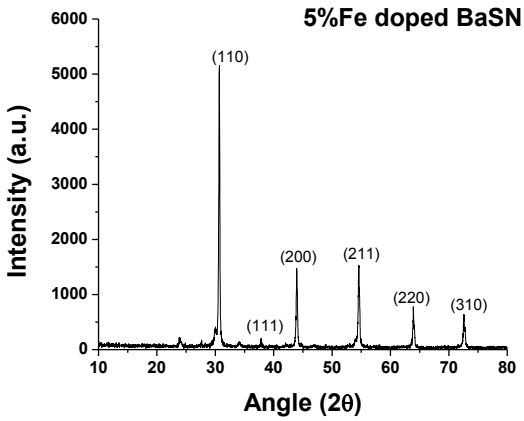

Fig 1: X-Ray diffraction pattern of 5% Fe doped $BaSnO_3$ powder sample

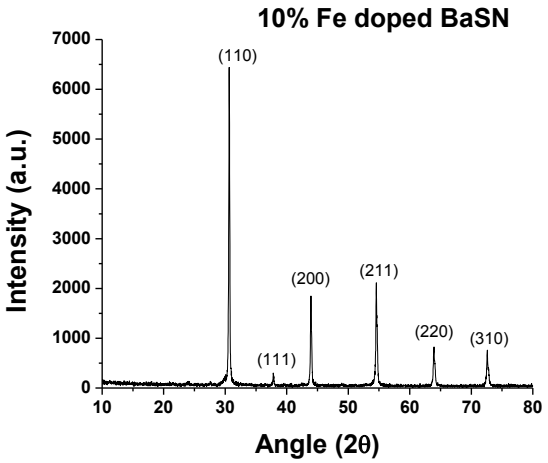

Fig 2: X-Ray diffraction pattern of 10% Fe doped $BaSnO_3$ powder sample

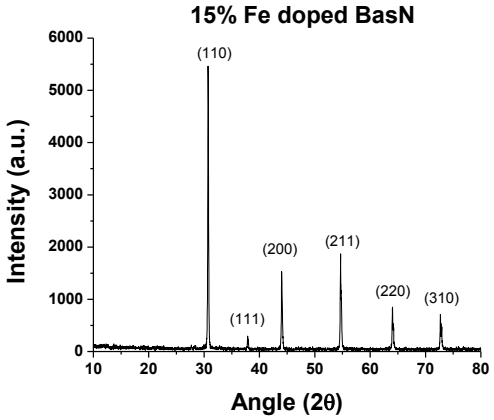

Fig 3: X-Ray diffraction pattern of 15% Fe doped $BaSnO_3$ powder sample

3.2. FTIR spectroscopy analysis

FTIR absorption spectra of the sample measured in the range between 400cm^{-1} to 5000cm^{-1} of Fe doped barium stannate with different composition have been shown in from Fig 4 to Fig 6. It has been observed that the Sn-O stretching vibration is observed at around 453 cm^{-1} and 645 cm^{-1} (Köferstein, Roberto *et. al.*) for all Fe doped samples. The bond is observed to be slightly decreased with increase in Fe dopant concentration. The dominant peak for all three composition at 645 cm^{-1} or 633 cm^{-1} represents (SnO_6) octahedral structure which has symmetrical stretching vibration (Omeiri S *et. al.*). The presence of small peak at 849 cm^{-1} and dominant peak at 1438 cm^{-1} for all three dopant composition have shown the existence of C-O stretching vibration (Omeiri S *et. al.*). Also these absorption band have shown the presence of characteristics band of $BaCO_3$ (Alves, C.F. Mary *et. al.*, M.W. Charles *et. al.*).

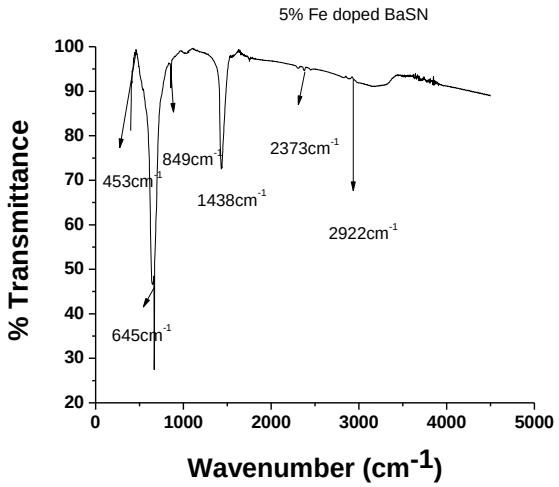

Fig 4: Fourier Transform Infrared spectrum of 5% Fe doped $BaSnO_3$

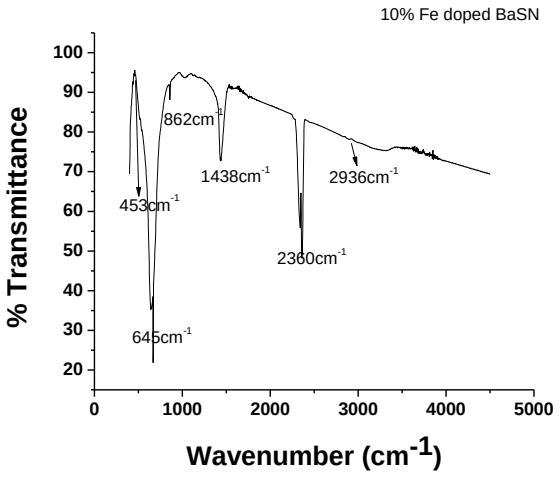

Fig 5: Fourier Transform Infrared spectrum of 10% Fe doped $BaSnO_3$

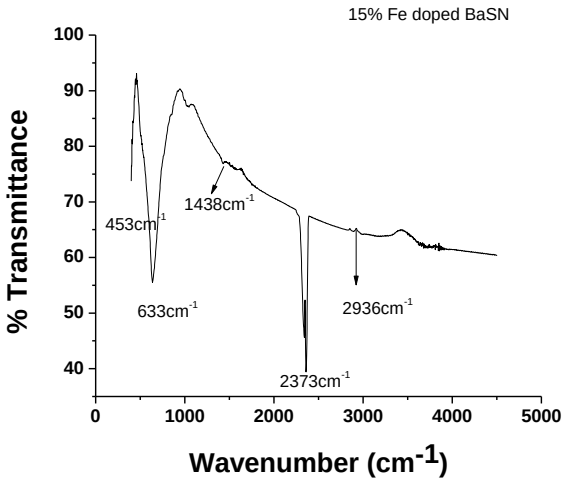

Fig 6: Fourier Transform Infrared spectrum of 15% Fe doped $BaSnO_3$

3.3. UV/VIS spectroscopy analysis

From UV-VIS spectral studies, absorbtion spectra of the sample is observed within the scan range between 200nm to 700nm for all Fe doped barium stannate samples with different concentration shown in the Figures 7 and 8. From these figures it has been shown that there are prominent absorption peak in the range between 200nm to 300nm while absorption is prominent in UV region compare to visible region (Vidya, S *et. al.*). The samples respond heavily in the ultra violet region and the optical absorption in the wavelength region lower than 400nm is mainly exhibited due to the electron transition from top of the valence band to the bottom of the conduction band (Yasukawa, Masahiro *et. al.*, M.W. Charles *et. al.*). Optical band gap energy or photon energy is determined by the Tauc's equation (Köferstein, Roberto *et. al.*). Direct band gap of material is given by Tauc relationship

$$\alpha(h\nu) = \mathbf{B}\,(h\nu - Eg)^m$$

where α is the absorption coefficient, B is an energy independent constant of the absorption coefficient**,** Eg is the optical band gap energy, h is the Planck's constant, ν is the frequency of incident photon and m is an index which depends on the nature of electronic transition responsible for the optical absorption, Values of m depends on direct and indirect transition which are respectively 1/2 and 2. Here the direct and indirect optical band gap energy measured of Fe doped barium stannate with different composition by physical routes are shown in Fig 9 to Fig10. Some paper revealed that band gap energy are in the range of 2eV to 3.4eV (Köfersteina, Roberto, Yakuphanoglub, Fahrettin., Bouhemadou, A *et. al.*). From Fig 9 it has been shown that for 5% Fe band gap energy of direct transition are 2.698eV consistent with reported data and band gap energy of indirect transition are 2.68eV closely in match with published literature. Band gap energy increases with increasing dopant concentration.

It may be due to possible defect levels generated within band energy structure leading to rise in activation energy required for electronic conduction jump from valence to conduction band. With rise in dopant concentration defect states get annihilated which leads to larger quantum level defects within band structure. For electronic conduction between the different generated energy level to the conduction band thus more driving potential is required in compare to simple electron-hole pair combinations. Hence, such rises in band gap energy level are observed for higher dopant concentration.

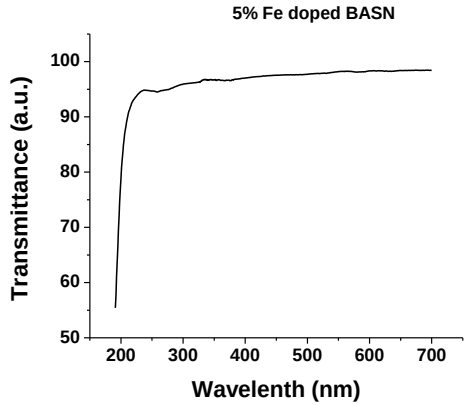

Fig 7: Absorption spectra of 5% Fe doped $BaSnO_3$ measured in the range from 200nm to 700nm

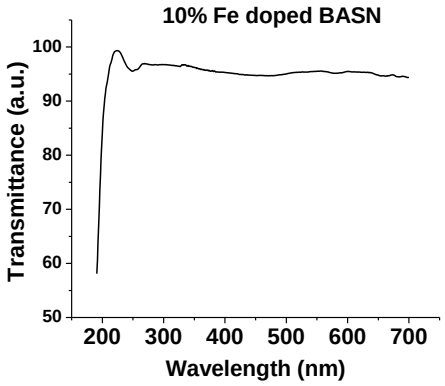

Fig 8: Absorption spectra of 10% Fe doped $BaSnO_3$ measured in the range from 200nm to 700nm

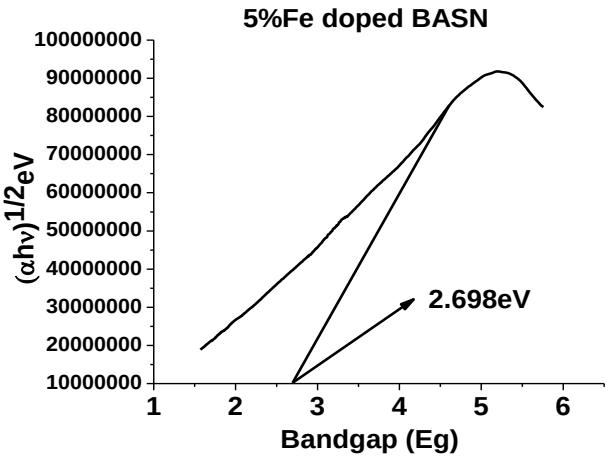

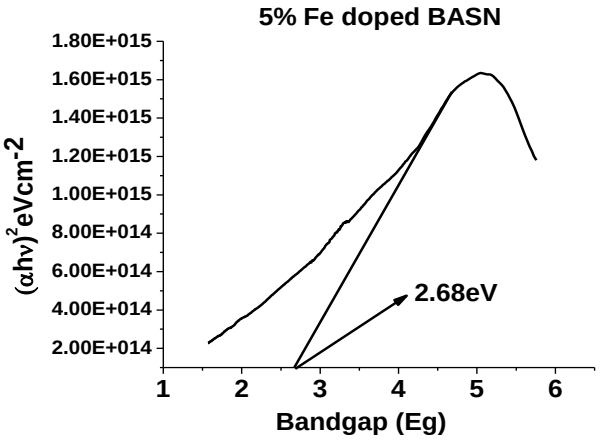

Fig 9: Plot of $(\alpha h\nu)^2$ and $(\alpha h\nu)^{1/2}$ of 5% Fe doped $BaSnO_3$ nanoparticles for direct and indirect transition

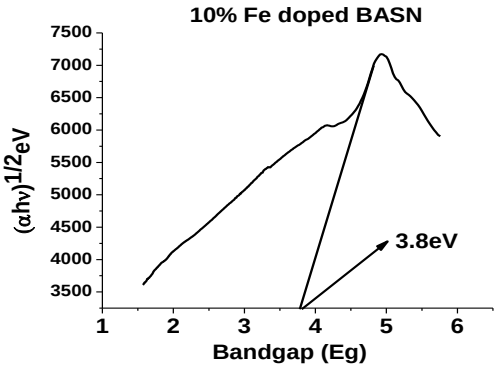

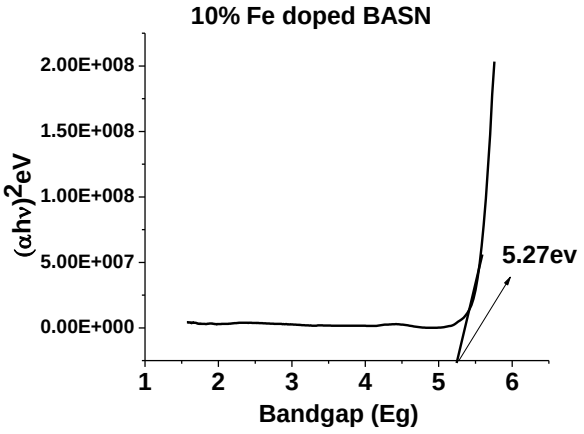

Fig 10: Plot of $(\alpha h\nu)^2$ and $(\alpha h\nu)^{1/2}$ of 10% Fe doped $BaSnO_3$ nanoparticles for direct and indirect transition

3.4. Microstructure and morphological Studies by SEM and elemental analysis by EDX

SEM and FESEM micrographs of Fe doped barium stannate $BaSn_{1-x}$ Fe_xO_3 with x= 0.05, 0.10 and 0.15 are shown in Fig 11 a-c and Fig 12 a-c. Micrographs of all the samples exhibit massive agglomerations with interconnection among particles. All the samples of Fe doped $BaSnO_3$ with different composition exhibits

interconnected agglomerates with no directional growth is observed. Some interconnected pores are also noted amongst the agglomerate structure where the individual grains are having cubical to spherical morphology. The average grain size for the samples with x=0.05 and x=0.1 is less than a 1μm[Yasukawa, Masahiro et. al.]. And the grain size for the samples with x=0.15 is almost nearly close to 1μm. So the variation of the grain size with different compositon of Fe doped $BaSnO_3$ is very small. The Figure 13 shows the results of EDX spectra for elemental analysis of synthesized material. The results confirmed the presence of the elements (Ba,Sn, Fe and O) in the calculated ratio responsible for the formation of required nano-crystalline perovskite compound.

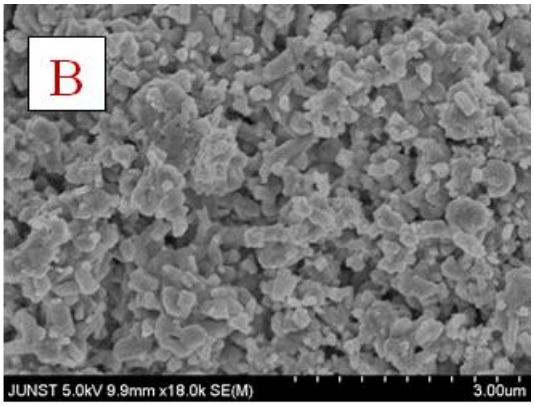

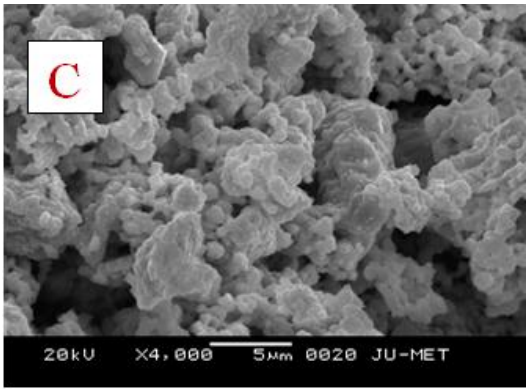

Fig 11: SEM images of $BaSn_{1-x}Fe_xO_3$ for (a) x=0.05 (b) x=0.10 (c) x=0.15

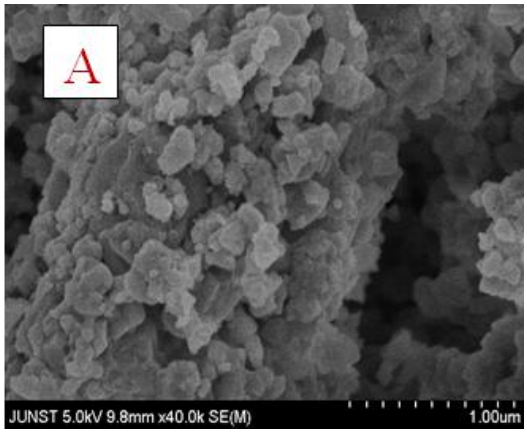

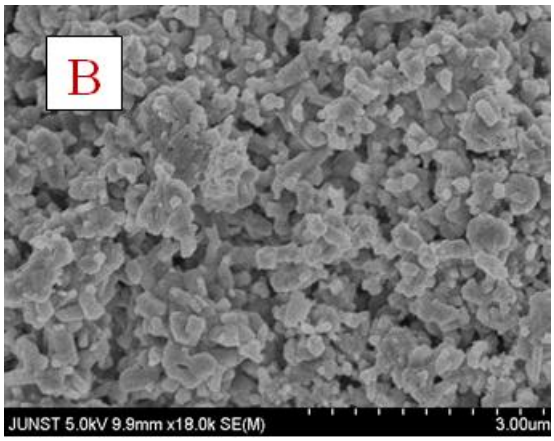

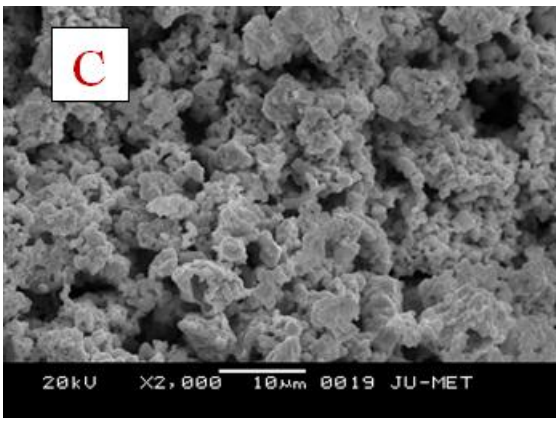

Fig 12: FESEM images of $BaSn_{1-x}Fe_xO_3$ for (a) x=0.05 (b) x=0.10 (c) x=0.15

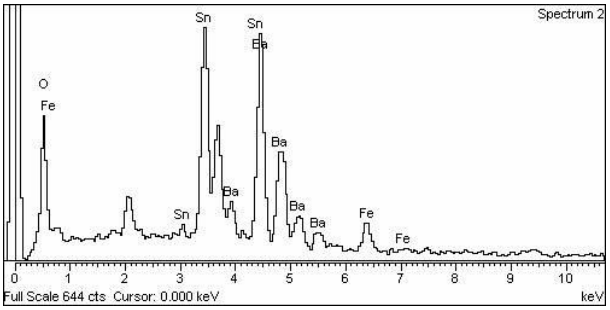

Fig 13: EDS spectra of $BaSn_{1-x}Fe_xO_3$ exhibiting spectra of elements present within the material

Conclusions

Iron (Fe) doped barium stannate i,e $BaSn_{1-x}Fe_xO_3$ with x= 0.05, 0.10 and 0.15 were prepared by mechanical mixing followed by sintering at 1350^0C for 2 hours using precursor $BaCO_3$, Fe_2O_3 and SnO_2. It has been observed that $BaSnO_3$ has a simple cubic perovskite type of structure with crystallite size around 49.12nm. The variation of crystallite size was found to be negligible with different composition of Fe doped $BaSnO_3$. Sn-O stretching vibration, C-O stretching vibration bands are noted from the FTIR spectral analysis. Sn-O stretching vibration bond is slightly decreased when we increase dopant concentrations. For all three compositions it is observed to have same

C-O stretching vibration bond. From UV-VIS analysis, it has been indicated that samples absorbs mostly in the UV region and no absorption in the visible region. For 5% Fe dopant band gap energy of direct transition are 2.698eV and band gap energy of indirect transition are 2.68eV. Band gap energy increases with increasing % of Fe composition due to annihilation of defect states within band structure level. Morphological studies by SEM revealed nature of granular formations and it is observed that grain size is less than 1μm. EDX analysis has confirmed the presence of elements responsible for the Iron doped Barium Stannate.

Acknowledgements

We are greatly indebted to Department of Metallurgical & Materials Engg, JU, Kolkata, India, for giving us the opportunity to take up this interesting project work. It is our privilege to convey our heartiest thanks to Mr. Sudhir Ghosh for supporting XRD facilities, Dr. Mrs. Jhimli Sarkar for UV-VIS, Mr. Jayanta Bhattacharya for SEM-EDX and Mr.Pankaj Bhadra for FTIR analysis.

References

Upadhyay, Shail., Parkash, Om., Kumar, Devendra., (2001), Solubility of lanthanum, nickel and chromium in barium stannate, *Materials Letter*, vol. 49, no.5, pp251–255.

Kocemba, I., Wróbel -Jedrzejewska, M., Szychowska, A., Rynkowski, J., Główka, M., (2007), The properties of barium stannate and aluminum oxide-based gas sensor The role of Al_2O_3 in this system, *Sensors & Actuators B-Chem*, vol.121, no.2, pp 401–405.

Lu, Wensheng., Schmidt, Helmut., (2008), Lyothermal synthesis of nanocrystalline $BaSnO_3$ powders. *Ceramic International*, vol.34**,** no.3, pp 645–649.

Köferstein, Roberto., Jäger, Lothar., Zenkner, Mandy., Müller, Thomas., Ebbinghaus, Stefan G., (2010), The influence of the additive BaGeO3 on BaSnO3 ceramics, *Journal of the European Ceramic Society*, vol.30, pp 1419–1425.

James, K.K., Aravind, Arun., Jayaraj, M.K**.,** (2013), Structural, optical and magnetic properties of Fe-doped bariumstannate thin films grown by PLD, *Applied Surface Science*, xxx (2013) xxx– xxx

Wei, Xiaoyong., Yao ,Xi., (2007), Preparation, structure and dielectric property of barium stannate titanate ceramics, *Materials Science and Engineering B*, vol.137, pp 184–188.

Upadhyay, Shail., Parkash, Om., Kumar, Devendra., (2007), Synthesis, structure and electrical behaviour of nickel-doped barium stannate, *Journal of Alloys & Compounds*, vol.432, no. 1-2, pp 258–264.

Bouhemadou, A., Haddadi, K., (2010), Structural, elastic, electronic and thermal properties of the cubic perovskite-type BaSnO3, *Solid State Sciences*, vol.12, pp 630–636.

Wei, Xiaoyong., Feng, Yujun., Hang, Lianmao., Xia, Song., Li Jin and Xi Yao, (2005), Abnormal *C–V* curve and clockwise hysteresis loop in ferroelectric barium stannate titanate ceramics, *Material Science and Engineering B-Solid*, vol.120**,** no**.** 1-3, pp. 64–67.

Singh, Prabhakar., Sebastian, Peter. C., Kumar, Devendra., Parkash, Om**,** (2007), Correlation of microstructure and electrical conduction behaviour with defect structure of niobium doped barium stannate, *Journal of Alloys & Compounds*, vol.437, no. 1-2, pp 34–38.

Omeiri, S., Hadjarab, B., Bouguelia, A., Trari, M., (2010), Electrical, optical and photoelectrochemical properties of BaSnO Applications to hydrogen evolution, *Journal of Alloys & Compounds*, vol.505, no. 2, pp 592–597.

Cullity, D. B, (1956) Elements of X-ray diffraction. (1956) A*ddison-wesley publishing company, inc.* reading, massachusetts pp 84**.**

Köferstein, Roberto., Abicht, Peter. Hans., Woltersdorf, Jörg., Pippel, Eckhard., (2006), Phase evolution of a barium tin 1,2-ethanediolato complex to barium stannate during thermal decomposition, *Thermochimia Acta*, vol.441, no**.**2, pp 176–183.

Alves, C.F. Mary., Souzaa, C. Soraia., Hebert H.S. Limaa, Marcelo R. Nascimentoa,b, Márcia R.S. Silvaa, JoséWaldo M. Espinosaa, Severino J.G. Limac, E. Longod, P.S. Pizanie, Luiz E.B. Soledadea, Antonio G. Souzaa, Iêda M.G. Santosa., (2009), Influence of the modifier on the short and long range disorder of stannate perovskites. *Journal of Alloys & Compounds*, vol.476, no.1-2, pp 507–512.

M.W. Charles, H. Nick Jr., E.S. Gregory., (1989) Physical Properties of Semiconductors. (1989) *Prentice-Hall, Englewood Cliffs, New Jersey* (49) Edition

Vidya, S., Rejith, P. P., John, Annamma., Solomon, Sam., Deepa, S. A., Thomas, J. K., (2011), Electrical, optical and vibrational characteristics of nano structured yttrium barium stannous oxide synthesized through a modified combustion method. *Materials Research Bulletin*, vol.46, no.10, pp 1723–1728.

Yasukawa, Masahiro., Kono,Toshio., Ueda, Kazushige., Yanagi, Hiroshi., Hosono, Hideo., (2010), High-temperature thermoelectric properties of La-doped BaSnO3 ceramics. *Materials Science and Engineering B*, vol.173, pp 29–32.

Köfersteina, Roberto., Yakuphanoglub, Fahrettin., (2010), Semiconducting properties of Ge-doped BaSnO3 ceramic. *Journal of Alloys and Compounds*. vol.506, pp 678–682.